ChemComm

This is an *Accepted Manuscript*, which has been through the Royal Society of Chemistry peer review process and has been accepted for publication.

Accepted Manuscripts are published online shortly after acceptance, before technical editing, formatting and proof reading. Using this free service, authors can make their results available to the community, in citable form, before we publish the edited article. We will replace this *Accepted Manuscript* with the edited and formatted *Advance Article* as soon as it is available.

You can find more information about *Accepted Manuscripts* in the **Information for Authors**.

Please note that technical editing may introduce minor changes to the text and/or graphics, which may alter content. The journal's standard **Terms & Conditions** and the **Ethical guidelines** still apply. In no event shall the Royal Society of Chemistry be held responsible for any errors or omissions in this *Accepted Manuscript* or any consequences arising from the use of any information it contains.

COMMUNICATION

Optimization of proton conductivity in graphene oxide by filling sulfate ion

Kazuto Hatakeyama,[ab] Mohammad Razaul Karim,[ac] Chikako Ogata,[ab] Hikaru Tateishi,[ab] Takaaki Taniguchi,[ab] Michio Koinuma,[ab] Shinya Hayami*[ab] and Yasumichi Matsumoto*[ab]

Graphene oxide (GO) walled channels filled by sulfate ion exhibit an optimized proton conductivity, which is higher than the proton conductivity of all other form of GO. The sulphate ion increases the water absorbing capacity and hydrogen bond reformation process in GO.

In a hydrogen fuel cell the transportation of proton from the hydrogen inlet to the oxygen chamber is supported by solid proton conductor.[1] The proton conductivities of GO and its derivatives have been reported only in recent years. GO contains various oxygenated functional groups, which can support the proton transportation through reformation of hydrogen bonds.[2] The proton conductivities of GO, its sulfonated derivatives, and hybrid with Nafion have been reported by various groups. Jung *et al.* reported that the proton conductivity of Nafion is possible to increase 5 times by doping 1% GO on it.[3] Zarrin *et al.* afforded to increase the conductivity in GO-Nafion composite by incorporating sulfonic acid group (HSO_3^{-}).[4] A moderately high proton conductivity of sulfonated GO paper was reported by Ravikumar *et al.*[5] But, the perfect inplane proton conductivity on single layer GO was reported by our group for the first time and the high proton conductivity of GO resulted from its extremely low thickness, flexible interlayer space, increased water content and the improved hydration dynamics.[6] In practice, the bulk sample is more desirable for fuel cell application. Therefore, it is necessary to optimize the proton conductivity in bulk samples by increasing the number of functional sites and the hydrophilicity.[6] Gao *et al.* synthesized ozonated GO, proton conductivity of which was 50% higher than virgin GO.[7] Further, we observed that in multilayer GO, the conductivity increases due to the increased hydration dynamics, flexible interlayer cavity and a wider pathway due to the option for the protons to travel through some nanopore oriented interlayer crossing.[8]

All these report implies that the proton conductivity in GO rises due to the improved water absorbing capacity and flexibility of the conduction channels. In opposite, the conductivity was found to decrease due to the blocking of epoxy sites by metal ions or by insertion of bulky hydrophilic groups at the GO moiety.[9, 10] Therefore, for further advancement in this field we avoided all attempts for formation of hybrids or functionalized GO, which can destroy or block the epoxy sites. As an alternative, herein we consider the insertion of hydrophilic sulfate ion at intercalated GO channels (sGO) to increase both the flexibility and hydrophilicity of the conduction tracks. Previously, the movement of small ions within nanofluidic GO channel was reported by Raidongia *et al.*[11] We show that the presence of H_2SO_4 at the interlayer results an optimized proton conductivity, which is higher than all forms of GO reported todate.

The image taken from atomic force microscope (AFM) and scanning electron microscope (SEM), energy dispersive spectra (EDS) and powder X-ray diffraction (PXRD) patterns in Fig. 1 confirm the presence of sulphate ions (SO_4^{2-}) or related products in sGO. The AFM height profile in Fig. 1a shows that the veins (3-100 nm), and hills (400-800 nm) of sGO samples are absent in GO. These swelled spots are clearly distinguishable from wrinkles and supposed to be generated from the presence of SO_4^{2-} or other related products at the interlayer. In Fig. 1b, the comparison between GO and sGO through EDS mapping and SEM images confirm the deposition of excess sulfur in the veins and hills. In addition, the XPS spectra confirm the presence of SO_4^{2-} ion in the sGO samples (Fig. S1, ESI†). The PXRD patterns in Fig. 1c represents that the inter layer distance for GO is 0.85 nm, whereas those for sGO samples are 1.7 and 1.2 nm with S / C (sulfur to carbon) atomic ratio as 0.41 and 0.08, respectively. These higher interlayer distances in sGO samples indicate the presence of bulky sulfate ions at interlayer. The inhomogeneous interlayer separation revelled from the broad diffraction peaks in sGO confirms the non uniform distribution of sulfate ion at interlayer. Fig. 1d represents the results for TGA analysis of sGO and GO (18 μm paper for both) at high and low RH. For sGO (with S / C ratio as 0.08) the water content is about 18 and 46 wt% at 30 and 90% RH, respectively. But, for GO at similar RH conditions the respective values are 21 and 31 wt%. Fig. 2a represents the Nyquist plots of various sGO samples, where the traces of the real (Z') and imaginary parts (Z") of impedance at each frequency were plotted and found to fit with distorted semicircular curves. Fig. 2b represents the RH dependent proton conductivities of GO, sGO samples, HCl leached GO and Nafion.[12, 13] The proton conductivities of sGO samples show some anomalous trend. At 20% RH the proton conductivity of virgin GO and sGO (SO_4^{2-}) film are 5×10^{-6} and 7×10^{-9} Scm^{-1}, respectively. The conductivities of other samples lie between these values. The rate of conductivity increment for sGO (SO_4^{2-}) is higher than all other sample. At $\approx$ 40% RH the
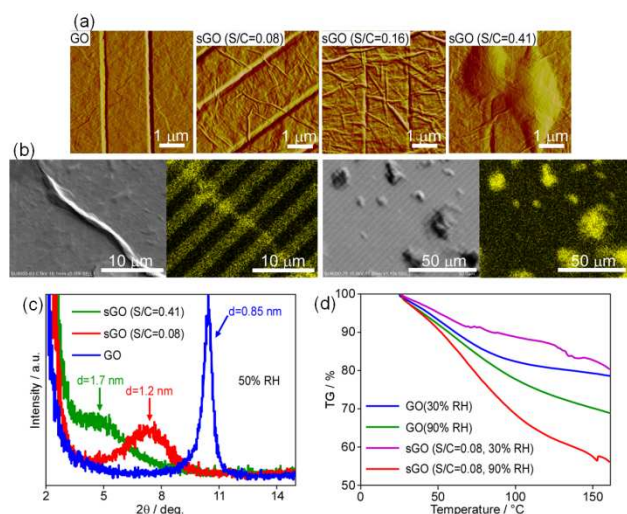
Fig. 1 (a) AFM images of multilayer GO and sGO films on the comb electrode surface (S / C atomic ratios of the sGO are described in parentheses). (b) SEM and EDS sulfur atom mapping images of sGO (S / C=0.41). Sulfate (SO_4^{2-}) is concentrated in the veins and hills. (c) XRD patterns of multilayer GO and sGO films under 50% RH (S / C atomic ratios of the sGO films are described in parentheses). (d) Weight losses due to the release of intercalated water of GO (18 μm) and sGO (S/C=0.08) samples. Before measurement the samples were incubated under 30 and 90% RH.

Fig. 2 (a) Nyquist plots for various samples. (b) Dependence of proton conductivities on RH (film thicknesses and S / C atomic ratios of the sGO films are described in parentheses). (c) Temperature dependent conductivities of various samples. (d) Dependence of the E_a values on RH (film thicknesses and S / C atomic ratios of the sGO films are described in parentheses).

conductivities of all samples are almost the same. The proton conductivity of sGO films undergoes a sudden increase at around 40% RH, above which the conductivities are much higher than GO, referred Nafion and GO-Nafion hybrids. HCl incorporation reduces the conductivity. The Na_2SO_4 loaded sample displays σ values almost equal to sGO at comparatively higher RH condition. The conductivity of GO film increases with the thickness.[8] Therefore, the higher conductivities of 120 and 170 nm sGO films (compared with 200 nm GO film) confirm the optimized proton conductivity in sGO. Fig. 2c shows that for sGO with higher sulfur content the conductivity is constant beyond 295 K. Other samples show almost constant conductivity. Fig. 2d shows that the RH dependent activation energy (E_a) is almost constant for proton conduction in GO, but is reduced gradually for proton conduction through Nafion and sGO films are. These results indicate that proton conduction in sGO is easier at high RH. The similar trend for sGO and Nafion implies some similarity in their proton conduction mechanism.

The reason behind high proton conductivity of nano scaled film was explained by Maier *et al.*[14] Maier considered the relation of ionic conductivity with space charge, charged non stoichiometries and defect chemistry. GO with nanometer ranged thickness follows the similar criteria suggested by Maier. According to Mayer's hypothesis for extremely thin films (L « 4λ, where L and λ are film thickness and Debye length, respectively), the conductivity increases with a very sharp steep up to certain thickness. Comparing the conductance of bulk sample and extremely thin LiCl films on sapphire, Maier predicted the possibility of amazingly high conductance for thin LiCl films.[15] But herein, the higher conductivity and anomalous behavior of sGO sample needs further explanation and reasoning.

First of all, the hydronium ion is the vehicle for proton transportation in GO materials. In our previous reports we observed lower conductivity of H_2O humidified samples for GO materials, which implies that the hydronium ions function as the carrier.[6, 8, 9, 10] Therefore, we explain the proton transportation in terms of the extant
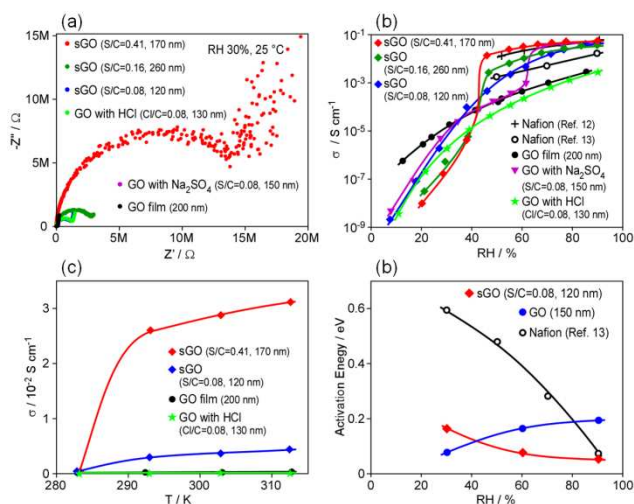
of water content, hydration behaviour and hydration dynamics inside the GO walled channels. From TGA measurement, sGO film had much larger amount of water than GO film. The carrier density of sGO film is much larger than GO film, and the higher proton conductivity is as per the expectation.

The proton conductivity is directly related to the amount of adsorbed water. In sGO, at high RH both the GO nanosheet and sulfate ion can adsorb water molecule. The functional sites of GO are hydrophilic. The SO_4^{2-} ion has a tetrahedral shaped resonance hybrid structure, where the four oxygen atoms contain partially negative charge. Therefore, SO_4^{2-} ion can be bonded with two opposite GO walls with or without water molecules. At high water content, two of the tetrahedron corner of SO_4^{2-} ion can bond to the moisture layer adsorbed to GO walls (Fig. 3a) and the remaining two sites become engaged with some interior water molecules. The overall water content is therefore higher than GO. The TGA data (Fig. 1d) suggests this fact. In reverse, at low water content two tetrahedron corners of SO_4^{2-} ion directly make bond with GO walls. Therefore, some break through within the continuity of humidified layer (Fig. 3b) lowers the proton conductivity. It seems that the 40% RH is somehow the threshold humidity to accommodate water molecule between two tetrahedron corner of SO_4^{2-} ion and GO walls. Therefore, the conductance shows a sharp steep around 40% RH. At low RH, instead of participating in proton transportation, the sulfate ions attribute some barrier within the conduction. It is clear from Fig. 1d that at 20% RH, the water content of sGO samples are much lower than that for GO. In addition at low RH, the conduction track in sGO is sluggish compared with GO, as the SO_4^{2-} ions function as some obstacle and destroy the continuity of adsorbed water layer. Therefore, the proton conductivities of sGO samples at low RH are significantly lower than that for GO. Also at low RH, the H^+ ion generated from the dissociation of intercalated acid molecules blocks some epoxy functional sites of GO, which ultimately damages the continuity of the conduction tracks. However, at high RH, this phenomenon becomes insignificant as the H^+ ions find available water molecules to form H_3O^+ ions. The low conductivity of HCl loaded sample also complies with this issue. The Na_2SO_4 loaded
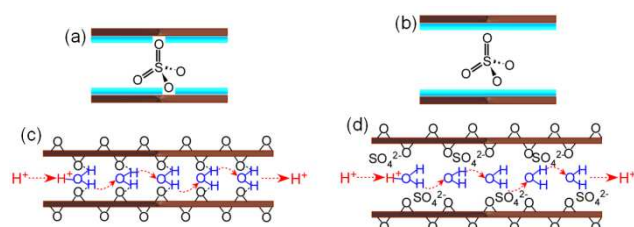
Fig. 3 (a) At low humidity the SO_4^{2-} ion is attached directly to the GO, the conduction channels is comparatively narrow as there is no water between a corner of tetrahedron and GO. The discontinuity of adsorbed water layer is also resulted (b) At high humidity condition there is water layer between the corner of sulfate tetrahedron and GO surface. The conduction channel is wider, and with continuity in adsorbed water layer. Propagation of H^+ ion through GO walls (c) and sGO film (d), respectively.

sample also exhibits higher conductivity due to the presence of sulfate ions. These sulfate ions behave as dilute sulfuric acid solution after reacting with additional amount of adsorbed water at high humidity. As the Na^+ ion blocks some of the epoxy sites of GO, a higher RH (ca 60%) is needed to solvolyse Na^+ ion for removing it from the epoxy sites. The dominance of proton conductivity was confirmed from isotope effect at low temperature. The conductivity of H_2O humidified GO is ~1.05 times higher than D_2O humidified GO (Fig. S2). The small sized H^+ ion posses significantly higher ionic mobility compared with Na^+. In GO materials the vehicle for conduction is the hydronium ion and the possibility for Na^+ ion to bond with H_2O to form a hydronium like ion is unfavorable considering the symmetry, charge balance and the asymmetric nature of the bonds. Almost a similar σ values for Na_2SO_4 and H_2SO_4 loaded GO, while a lower conductivity for HCl loaded sample confirms that in sGO films the sulfate ions plays the major role to increase the conductivity.

The second factor behind the anomalous and high conductivity of sGO is the flexibility of GO channels attributed by SO_4^{2-} ion. The hydration phenomenon and water dynamics for oxidized graphitic materials were reported previously by several groups.[16] In sGO, the bulky SO_4^{2-} ion makes the interlayer space swelled and more separated. At low RH the SO_4^{2-} ion is directly bonded to two opposite GO surface and the flexibility of the channel is low. At higher humidity, the water layers between the SO_4^{2-} ion and GO wall makes the channels wider and more flexible. Sulfuric acid transfers protons through hydrogen-bonded network at low concentrations.[17] The constant E_a value for GO (Fig. 2d) matches with some previous report. But for sGO films, the E_a value decreases with RH and matches with that for Nafion. Therefore, we propose that along with the fundamental advantage provided by GO, the proton conduction of sGO also is governed by sulfuric acid filled within it. The structure of sGO film is comparable with Nafion. In Nafion some hydrophilic $-SO_3^-$ functional groups are present, whereas in sGO there exist some oxygenated functional sites and intercalated sulfate ion. The perspective proton transfer mechanism in Fig. 3c and 3d shows that in GO and sGO proton mobility and hydrogen bond reformation is supported by double GO walls and attached water molecules. But, the conduction pathway is wider and in sGO. We also studied the effect of H_2SO_4 concentration on the conductivities of sGO films. With relatively large amounts of H_2SO_4, the proton conductivities remarkably increased beyond 40% RH.

In conclusion, the morphological study confirms the presence of sulfate ion at the interlayer. At low RH the proton conductivity of sGO is lower, but above 40% RH the conductance radically exceeds that for all GO materials reported todate. The TGA analysis show that the water content of sGO is lower and higher than virgin GO

sample at low and high RH, respectively. The displayed veins and hills in sGO imply increased distances between two opposite GO walls. In combination with high water content and increased flexibility the conductivity of sGO samples reach to an optimized value. We are looking forward to use sGO in fuel cells.

Notes and references

[a] Graduate School of Science and Technology, Kumamoto University, 2-39-1 Kurokami, Chuo-ku, Kumamoto 860-8555, Japan.
E-mail: yasumi@gpo.kumamoto-u.ac.jp, Hayami@sci.kumamoto-u.ac.jp; Fax: +81-96-342-3679; Tel: +81-96-342-3659
[b] JST, CREST, Gobancho, 7 Gobancho, Chiyoda-ku, Tokyo, 102-0076, Japan.
[c] Department of Chemistry, School of Physical Sciences, Shahjalal University of Science & Technology, Sylhet-3114, Bangladesh
† Electronic Supplementary Information (ESI) available: Experimental details and XPS spectra. See DOI: 10.1039/c000000x/

1 G. A. Voth, *Acc. Chem., Res.* 2006, **39**, 143-150.
2 (a) M. Acik, C. Mattevi, C. Gong, G. Lee, K. Cho, M. Chhowalla and Y. J. Chabal, *ACS Nano*, 2010, **4**, 5861-5868; (b) Y. W. Zhu, S. Murali, W. W. Cai, X. S. Li, J. W. Suk, J. R. Potts and R. S. Ruoff, *Adv. Mater.*, 2010, **22**, 3906-3924.
3 J. H. Jung, J. H. Jeon, V. Sridhar and I. K. Oh, *Carbon*, 2011, **49**, 1279-1289.
4 H. Zarrin, D. Higgins, Y. Jun, Z. W. Chen and M. Fowler, *J. Phys. Chem. C*, 2011, **115**, 20774-20781.
5 Ravikumar and K. Scott, *Chem. Commun.*, 2012, **48**, 5584-5586.
6 M. R. Karim, K. Hatakeyama, T. Matsui, H. Takehira, T. Taniguchi, M. Koinuma, Y. Matsumoto, T. Akutagawa, T. Nakamura, S. Noro, T. Yamada, H. Kitagawa and S. Hayami, *J. Am. Chem. Soc.*, 2013, **135**, 8097-8100.
7 W. Gao, G. Wu, M. T. Janicke, D. A. Cullen, R. Mukundan, J. K. Baldwin, E. L. Brosha, C. Galande, P. M. Ajayan, K. L. More, A. M. Dattelbaum and P. Zelenay, *Angew. Chem., Int. Ed.*, 2014, **53**, 3588-3593.
8 K. Hatakeyama, R. Karim, Mohammad, C. Ogata, H. Tateishi, A. Funatsu, T. Taniguchi, M. Koinuma, S. Hayami and Y. Matsumoto, *Angew. Chem., Int. Ed.*, 2014, **53**, 6997-7000.
9 Y. Ikeda, M. R. Karim, H. Takehira, T. Matsui, K. Hatakeyama, Y. Murashima, T. Taniguchi, M. Koinuma, M. Nakamura, Y. Matsumoto and S. Hayami, *Bull. Chem. Soc. J.*, 2014, **87**, 639-641.
10 Y. Ikeda, M. R. M. R. Karim, H. Takehira, T. Matsui, T. Taniguchi, M. Koinuma, Y. Matsumoto and S. Hayami, *Chem Lett.*, 2013, **42**, 1412-1414.
11 K. Raidongia and J. Huang, *J. Am. Chem. Soc.*, 2012, **134**, 16528-16531.
12 Y. Sone, P. Ekdunge and D. Simonsson, *J. Electrochem. Soc.*, 1996, **143**, 1254.
13 B. Dong, L. Gwee, D. Salas-de la Cruz, K. I. Winey and Y. A. Elabd, *Nano Lett.*, 2010, **10**, 3785-3790.
14 (a) J. Maier, *Solid State Ionics*, 1987, **23**, 59-67; (b) J. Maier, *Solid State Ionics*, 2003, **157**, 327-334.
15 E. Schreck, K. Läuger and K. Dransfeld, *Z. Phys. B: Condens. Matter.*, 1986, **62**, 331-334.
16 (a) A. Buchsteiner, A. Lerf and J. Pieper, *J. Phys. Chem. B*, 2006, **110**, 22328-22338; (b) S. Cerveny, F. Barroso-Bujans, A. Alegria and J. Colmenero, *J. Phys. Chem. C*, 2010, **114**, 2604-2612; (c) A. Lerf, A. Buchsteiner, J. Pieper, S. Schottl, I. Dekany, T. Szabo and H. P. Boehm, *J. Phys. Chem. Solids*, 2006, **67**, 1106-1110.
17 V. M. Gun'ko, V. V. Turov, R. L. D. Whitby, G. P. Prykhod'ko, A. V. Turov and S. V. Mikhalovsky, *Carbon*, 2013, **57**, 191-201.